Since January 2020 Elsevier has created a COVID-19 resource centre with free information in English and Mandarin on the novel coronavirus COVID-19. The COVID-19 resource centre is hosted on Elsevier Connect, the company's public news and information website.

VIROLOGY 177, 646–656 (1990)

Establishing a Genetic Recombination Map for Murine Coronavirus Strain A59 Complementation Groups

RALPH S. BARIC,*,[1] KAISONG FU,* MARY C. SCHAAD,* AND STEPHEN A. STOHLMAN†

*Department of Parasitology and Lab Practice, School of Public Health, University of North Carolina at Chapel Hill, Chapel Hill, North Carolina 27599-7400; and †Department of Neurology and Microbiology, University of Southern California, School of Medicine, 2025 Zonal Avenue, Los Angeles, California 90007

Received December 7, 1989; accepted April 20, 1990

MHV-A59 temperature-sensitive mutants, representing one RNA$^+$ and five RNA$^-$ complementation groups, were isolated and characterized by genetic recombination techniques. Maximum recombination frequencies occurred under multiplicities of infection greater than 10 each in which 99.99% of the cells were co-infected. Recombination frequencies between different ts mutants increased steadily during infection and peaked late in the virus growth cycle. These data suggest that recombination is a late event in the virus replication cycle. Recombination frequencies were also found to range from 63 to 20,000 times higher than the sum of the spontaneous reversion frequencies of each ts mutant used in the cross. Utilizing standard genetic recombination techniques, the five RNA$^-$ complementation groups of MHV-A59 were arranged into an additive, linear, genetic map located at the 5′ end of the genome in the 23-kb polymerase region. These data indicate that at least five distinct functions are encoded in the MHV polymerase region which function in virus transcription. Moreover, using well-characterized ts mutants the recombination frequency for the entire 32-kb MHV genome was found to approach 25% or more. This is the highest recombination frequency described for a nonsegmented, linear, plus-polarity RNA virus.

INTRODUCTION

Temperature-sensitive (ts) mutants of animal viruses have been used to elucidate many of the basic mechanisms of virus transcription, replication, assembly, and release in eukaryotic cells. Not surprisingly, ts mutants have been described for most oncogenic and nononcogenic RNA and DNA viruses (Fenner, 1970; Ghendon, 1972). The gene order for several DNA-containing viruses has been established by DNA recombination analysis utilizing ts mutants and standard genetic techniques (Epstein *et al.*, 1963; Ghendon, 1972; Ritchie, 1973). Among those RNA viruses possessing segmented genomes, intercistronic reassortment between wild-type or ts genome segments has identified the location and function of many reovirus, bunyavirus, and influenza virus genes (Fields, 1981). Reassortment frequencies for the influenza viruses and reoviruses vary from 2 to 42% depending on the virus strain and genome segment (Fields and Joklik, 1969; Fields, 1981; Scholtissek *et al.*, 1978).

Evidence for homologous RNA recombination among RNA viruses with nonsegmented genomes has been reported for polioviruses, apthoviruses, and coronaviruses (Cooper, 1968; Lai *et al.*, 1985; Lake *et al.*, 1975; Mackenzie *et al.*, 1975). Recombination frequencies between poliovirus ts mutants approach 2.2% or roughly 1% per 1700 nucleotide pairs of double-stranded RNA (Cooper 1968, 1977; Cooper *et al.*, 1975). Poliovirus recombination probably occurs during negative strand RNA synthesis by a copy choice mechanism (Kirkegaard and Baltimore, 1986); however, the apthovirus and coronavirus recombination mechanisms are unclear. Numerous RNA recombinant viruses of mouse hepatitis virus (MHV), a member of the Coronaviridae, have been isolated and characterized by T1 fingerprint analysis or sequencing of crossover sites (Keck *et al.*, 1987, 1988b; Lai *et al.*, 1985). Among different MHV strains, a region of polymorphism and deletion has been detected in the MHV S glycoprotein gene (Parker *et al.*, 1989). A high frequency of RNA recombination has been suggested previously, but an exact frequency for the entire MHV genome has not been determined (Makino *et al.*, 1986b). Analysis of MHV-infected cells has revealed the presence of discrete RNA products bound to and dissociated from the replicative intermediate RNA which might represent transcription and RNA recombination intermediates (Baric *et al.*, 1983, 1985, 1987). The precise role of these intermediates in transcription and recombination has yet to be determined. Sequence analysis also suggests that nonhomologous recombination between wild-type MHV and influenza C virus may occur during mixed infection (Luytjes *et al.*, 1988). The mechanism for nonhomologous recombination is unclear.

[1] To whom reprint requests should be addressed.

0042-6822/90 $3.00

Recombination between the genomes of nonsegmented RNA viruses provides a convenient tool to map the genetic loci of individual ts lesions and viral genes. Utilizing standard genetic recombination techniques, poliovirus and apthovirus ts mutants have been arranged into an additive, linear, genetic map with mutants at different locations differing in physiologic function (Cooper *et al.*, 1975; Lake *et al.*, 1975). This has permitted the localization of many structural and nonstructural gene functions to particular proteins. Temperature sensitive mutants of MHV have been isolated and characterized by complementation analysis and RNA phenotype (Koolen *et al.*, 1983; Leibowitz *et al.*, 1982; Martin *et al.*, 1988; Schaad *et al.*, 1990). Utilizing the ts mutants described in the accompanying manuscript (Schaad *et al.*, 1990) and standard genetic recombination techniques, we have formulated the first additive, linear, genetic map for MHV-A59 ts mutants. These data suggest that five or more genetic functions are encoded at the 5′ end of the genome which participate in regulating RNA synthesis. Moreover, utilizing well-characterized ts mutants from different complementation groups, our data suggests that the actual recombination frequency for the MHV genome may approach 25%. This is the highest homologous RNA recombination frequency reported for a nonsegmented RNA virus.

METHODS

Virus propagation and assay procedures

Temperature sensitive mutants representing one RNA^+ and five RNA^- complementation groups of MHV-A59 were used throughout the course of this study. Virus stocks were propagated at 32° in 150-cm^2 flasks containing DBT cells as described in the accompanying paper (Schaad *et al.*, 1990). Conditional lethal mutants used in this study represent the RNA^- complementation group A (LA3, LA6, LA16, NC8); group B (LA16, NC2, NC11); group C (LA8, LA9, NC1, NC10); group D (LA10); and group E (LA18, NC4, NC12). The group F RNA^+ mutants used in this study include LA7 and LA12. Plaque assays were performed at 32 or 39.5° in Dulbecco's modified essential medium (DMEM) (Sigma) in DBT cells containing 10% Nu-serum (Collaborative Research Inc.), 1% antibiotic/antimycotic (GIBCO), and 0.8% agarose. All plaque assays were quantified by staining with neutral red for 2 hr at 28–36 hr postinfection.

Recombination test

To map the location and orientation of the MHV complementation groups, a modification of the approach previously described to map the location of the poliovirus and apthovirus ts mutants was developed (Cooper *et al.*, 1975; Lake *et al.*, 1975; Mackenzie *et al.*, 1975). Cultures of DBT cells were seeded at a density of 1×10^6 cells/well (Falcon 6 well plate) in DMEM containing 10% Nu-serum and 1% antibiotic/antimycotic. Combinations of ts mutants were mixed and inoculated onto DBT cells at a m.o.i. of 10 for each mutant. Virus was adsorbed for 1 hr at room temperature and the inoculum removed. Individual wells were washed gently two times with 2 ml of warm PBS to remove unbound virus, and incubated at 32° for 16 hr in 2 ml of DMEM containing 10% Nu-serum and 1% antibiotic/antimycotic. Virus progeny were harvested and frozen at −70°. Each cross was titered at both 32 and 39.5° by plaque assay and the recombination frequencies were calculated as the percentage of ts^+ virus present in the progeny from the following formula (Lake *et al.*, 1975; Mackenzie *et al.*, 1975):

$$\mathrm{RF} = \frac{(AB)_{39.5} - (A + B)_{39.5}}{(AB)_{32}} \times 100.$$

$(AB)_{39.5}$ was the titer of the cross at the nonpermissive temperature while $(AB)_{32}$ represents the titer of the same cross at permissive temperature. $(A + B)_{39.5}$ was the sum of the revertants of each parent strain assayed at the restrictive temperature. This particular approach allows recombination to occur without selective pressure at 32° and provides a more realistic assessment of the true recombination frequency by calculating the percentage of ts^+ virus present within a given population. The formula only measures single crossover events resulting in the ts^+ phenotype and does not account for recombination events in the opposite direction resulting in the double ts mutant phenotype.

Recombination frequencies were compared to a reference cross (LA7 × LA9) that was included in each experiment to obviate day to day variations. These mutants were chosen for study because they have low reversion frequencies and the mutations in LA7 and LA9 have been mapped by T1 fingerprint analysis (Lai *et al.*, 1985; Makino *et al.*, 1986b, 1987). Day to day variations in recombination frequencies were standardized with the following formula:

$$\frac{(A_{\mathrm{std}})(xB_{\mathrm{exp}})}{(xA_{\mathrm{exp}})} = B_{\mathrm{std}}.$$

A_{std} was the mean recombination frequency of the reference cross LA7 × LA9 that was calculated from 12 replicative crosses. xB_{exp} was the mean recombination frequency of the two ts mutants being standardized to the reference cross and xA_{exp} was the recombination frequency of the standard cross (LA7 × LA9) that had been calculated during this particular experiment. B_{std}

was the standardized recombination frequency of cross *B*.

Construction of a MHV-A59 genetic recombination map

The average recombination frequency for each cross was calculated by standardizing 5 to 10 individual crosses to the control cross (LA7 × LA9). Standard deviations were calculated for each cross and the map locations positioned with respect to LA7 and LA9. Following analysis of recombinant virus by ts^+ phenotype, the mutants were arranged according to standard genetic practice assuming (1) recombination events were proportional to the distance between alleles; (2) double crossover events were a rarity as compared to single crossover events. Previous data with apthovirus and poliovirus ts mutants support the validity of these assumptions (Cooper *et al.*, 1975; Cooper, 1977; Lake *et al.*, 1975; Mackenzie *et al.*, 1975).

RESULTS

Effect of the input multiplicity on the MHV-A59 recombination frequency

Previous studies with apthoviruses and polioviruses clearly demonstrated that the input multiplicity of infection dramatically affects the final recombination frequency of a particular cross (Lake *et al.*, 1975; Mackenzie *et al.*, 1975). These studies demonstrated that as the m.o.i. decreased, recombination frequencies decreased accordingly. Polioviruses and apthoviruses cause cytopathic rounding of infected cells while MHV-A59 causes fusion and giant cell formation (Spaan *et al.*, 1988). This feature of MHV-A59 infection could dramatically alter the effect of input multiplicity on the final recombination frequency of a particular cross by allowing recombination between singly infected cells to occur following fusion. To assess the effect of cell fusion and optimize the input multiplicity for maximum recombination frequencies, cells were inoculated with ts LA7 and LA9 at varying multiplicities of infection and maintained at 32°. Progeny were harvested at 16 hr postinfection and titered at both the permissive and nonpermissive temperatures. In general, recombination frequencies were highest at m.o.i.s greater than 1.25 in which over 50% of the cells were co-infected with both ts mutants (Table 1). However, the most consistent results were obtained with m.o.i.s greater than 5. In contrast to results obtained with poliovirus and apthoviruses, recombination frequencies for MHV-A59 remained relatively high at input multiplicities in which only 7% of the cells were co-infected (m.o.i.—0.31) (Table 1). While direct evidence is lacking, the most likely interpretation from these data is that coronavirus RNA recombination is a late event in the viral growth cycle which can occur after fusion of singly infected cells.

TABLE 1

EFFECTS OF MULTIPLICITY OF INFECTION ON INTERTYPIC MHV RNA RECOMBINATION FREQUENCY

m.o.i.		Theoretical % of cells mixedly infected[a]	Recombination frequency[b]
ts LA9	LA7		
20.00	20.00	100.00	4.82 ± 0.60
10.00	10.00	100.00	3.38 ± 0.10
5.00	5.00	98.70	4.07 ± 1.71
2.50	2.50	84.30	3.26 ± 0.90
1.25	1.25	50.90	4.28 ± 1.77
0.62	0.62	21.30	2.61 ± 1.60
0.31	0.31	7.10	1.53 ± 0.60
0.16	0.16	2.20	0.81 ± 0.10
0.08	0.08	0.60	0.49 ± 0.04
0.04	0.04	0.15	0.07 ± 0.02
0.02	0.02	0.04	ND[c]
0.01	0.01	0.01	ND
20.00	10.00	100.00	3.21 ± 0.50
20.00	5.00	99.30	3.83 ± 0.40
20.00	2.50	91.80	1.44 ± 0.50
20.00	1.25	71.30	0.61 ± 0.01
20.00	0.62	46.20	0.61 ± 0.05
20.00	0.10	9.50	0.05 ± 0.02

[a] Calculated from the formula $(1 - e^{-Ma})(1 - e^{-Mb})100$, where Ma and Mb are input multiplicities.

[b] Calculated from the formula $RF = \frac{(AB)_{39.5} - (A + B)_{39.5}}{(AB)_{32}} \times 100$; where $AB_{39.5}$ is titer at nonpermissive temperature, $A + B_{39.5}$ is the sum of the reversion frequencies, and AB_{32} is titer of the cross at permissive temperature.

[c] Not detected.

Time course for the release of MHV-A59 recombinant virus

Previous studies with poliovirus indicate that the appearance of recombinant ts^+ virus during a single growth cycle peaks early in infection and remains constant until the death of the cell (Lake *et al.*, 1975; Mackenzie *et al.*, 1975). These data suggest that poliovirus recombination occurs early in the virus growth cycle. It is unclear whether recombinant viruses are released early or late in the MHV-A59 infectious cycle. To address this question, recombination frequencies were calculated at different times in the virus growth cycle from duplicate samples of the cross LA16 × LA18, LA6 × LA16, and NC2 × LA7. These mutants were chosen since they were of the RNA^- phenotype and represent members in the same (LA6 and LA16—group A) or

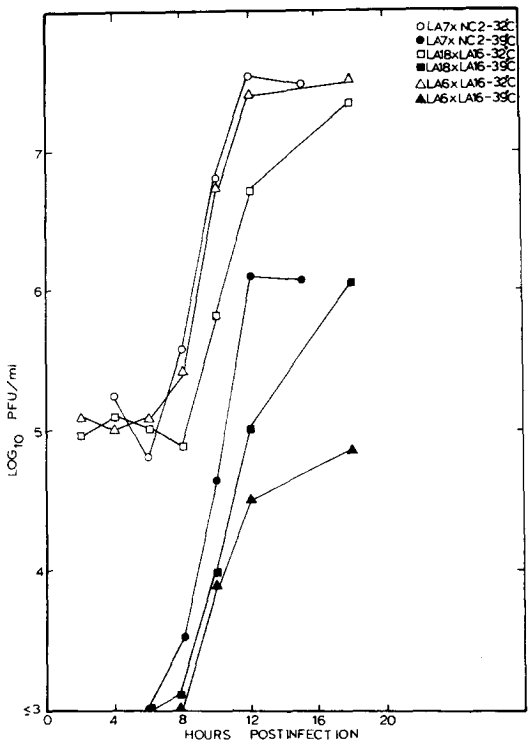

FIG. 1. Growth curves during mixed-MHV infection. Cultures of cells were infected at a m.o.i. of 10 each with two ts mutants representing the same or different RNA$^-$ complementation group of MHV-A59. After 1 hr for adsorption, the monolayers were washed, media replaced, and incubated at 32° for 16–18 hr. Virus progeny were harvested at different times postinfection and titered by plaque assay at permissive or nonpermissive temperatures. Virus titers: LA6 × LA16—32°, △; 39° ▲. LA16 × LA18—32°, □; 39° ■. NC2 × LA7—32°, ○; 39° ●.

different (LA18—group E; NC2—group B; LA7—group F) complementation groups. The double mutant LA16 (group A/B) was used because of the low reversion frequency of this mutant at restrictive temperature. Cultures of cells were co-infected with two ts mutants at a m.o.i. of 10 each and maintained at 32°. Virus titers were analyzed at different times postinfection at the permissive or restrictive temperatures. At 32°, all crosses replicated to virtually identical titers and were characterized by similar growth kinetics. However, the percentage of ts$^+$ virus was significantly higher between mutants of different complementation groups (LA16 × LA18, and NC2 × LA7) (Fig. 1). The peak recombination frequency was 5.05% between complementation groups A/B and E (LA16 × LA18), 5.95% between groups B and F (NC2 × LA7), and 0.2% between members of the same complementation group A (LA6 × LA16). In contrast to results reported for poliovirus, coronavirus recombination frequencies increased throughout infection and peaked between 16 and 18 hr postinfection (Fig. 2). These data further suggest that MHV-A59 recombination may be a late event in the virus growth cycle.

Recombination versus reversion frequencies

To assess the difference between the recombination versus reversion frequency, we performed a series of crosses between ts mutants representing different complementation groups of MHV-A59. The ratio of recombinants/revertants ranged from 63 to 20,000 times higher than the sum of the spontaneous reversion frequency of each individual mutant (Table 2). The extent of the difference reflected both the stability of the mutants used in the cross and whether the mutants were members of the same or different complementation groups. Between different complementation groups, recombination frequencies between individual mutants were as much as 10-fold higher than those previously reported for either polioviruses or apthoviruses, and support previous findings suggesting that high fre-

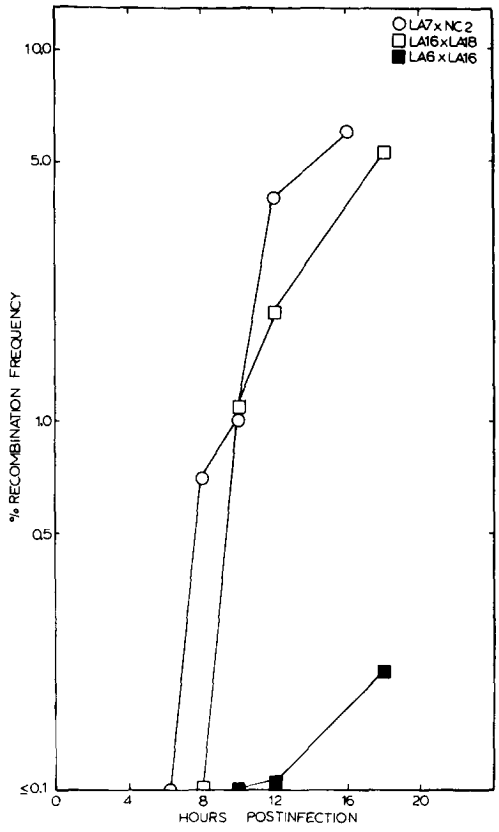

FIG. 2. Time course for the release of RNA recombinant viruses. Cultures of DBT cells were infected at a m.o.i. of 10 each with two different ts mutants as described in the legend to Fig. 2. RNA recombination frequencies were calculated by subtraction of reversion frequencies from singly infected cells as described under Methods. LA6 × LA16, □; LA16 × LA18, ■; NC2 × LA7, ○.

TABLE 2

RECOMBINATION VS REVERSION FREQUENCY DURING MIXED-MHV INFECTION

Mutant	32°	39°	Reversion frequency[a]	RF[b]	Proportion[c]
LA3	9.0×10^7	1.0×10^2	1.1×10^{-5}	—	—
LA6	8.5×10^7	4.1×10^4	4.8×10^{-4}	—	—
LA7	5.5×10^7	1.0×10^2	1.8×10^{-6}	—	—
LA9	8.6×10^7	7.8×10^3	9.0×10^{-4}	—	—
LA10	5.6×10^7	2.7×10^4	2.7×10^{-4}	—	—
LA18	1.0×10^1	1.9×10^6	5.3×10^{-6}	—	—
7 × 3	4.4×10^7	4.0×10^6	—	9.1	20,000
7 × 6	9.6×10^7	8.5×10^6	—	8.9	207.0
7 × 9	9.7×10^7	4.0×10^6	—	4.1	512.0
7 × 10	6.5×10^7	1.7×10^6	—	2.6	63.0
7 × 18	2.9×10^7	2.4×10^5	—	0.8	2,182.0

[a] Calculated as 39°/32°.
[b] Recombination frequency calculated as described under Methods.
[c] Proportion is the number of ts^- recombinant viruses divided by the number of revertant viruses titered at 39° from singly infected cells.

quency recombination occurs during mixed MHV infection (Keck *et al.*, 1987, 1988b; Makino *et al.*, 1986b).

Obstacles to mapping the location of the MHV-A59 complementation groups

To obtain a mean recombination frequency for a standard cross, we chose two mutants whose genetic defects had been mapped by recombination studies. Complementation group E mutant LA7 maps 7 to 8KB from the 3′ end of the genome in the S envelope glycoprotein gene while group C mutant LA9 maps at the 5′ end of the genome in the putative polymerase gene (Lai *et al.*, 1985; Makino *et al.*, 1986b, 1987). The mean recombination frequency of the standard cross was obtained from 12 replicated crosses of LA7 × LA9 with a mean recombination frequency of 4.45 + 0.85 (Table 3). To minimize day to day variations, crosses performed on different days included the standard cross (Table 3).

Construction of a genetic recombination map for MHV-A59 complementation groups

In contrast to studies with poliovirus and apthovirus ts mutants, MHV-A59 ts mutants are amenable to complementation analysis (Koolen *et al.*, 1983; Leibowitz *et al.*, 1982; Schaad *et al.*, 1990) permitting the recognition of distinct gene functions and facilitating genetic mapping. Unique ts mutants, isolated from different mutagenesis experiments, were selected from each complementation group and crossed with the reference mutants LA7 or LA9. In addition, mutants from each complementation group were also crossed with mutants representing all other complementation groups. The recombination frequencies and standard deviations for each cross are summarized in Table 4. The distances between complementation groups are within statistical limits and permit the construction of a genetic map (Fig. 3). In support of findings presented in the accompanying paper, ts mutants from each

TABLE 3

EFFECT OF STANDARDIZATION ON MHV RECOMBINATION FREQUENCIES

Standard LA7 × LA9 recombination frequency[a]		Before standardization[b]	Following standardization[c]
	Experiment 1		
4.277	LA7 × LA9	3.77	4.45
4.102	LA7 × LA10	2.30	2.70
4.448	LA7 × LA18	0.81	0.95
5.714			
3.750	Experiment 2		
3.980	LA7 × LA9	4.24	4.45
4.226	LA7 × LA10	1.56	1.67
3.425	LA7 × LA18	1.46	1.53
5.700			
3.499			
6.025			
4.170			
4.445 ± 0.845			

[a] Observed mean of 12 replicated crosses.
[b] Observed mean of 3 replicated crosses.
[c] Standardized against LA7 × LA9 by the formula $\frac{(A_{std})(xB_{exp})}{(xA_{exp})} = B_{std}$, where A_{std} is the standard recombination frequency of LA7 × LA9, xA_{exp} is the recombination frequency of LA7 × LA9 cross in the experiment; xB_{exp} is the recombination frequency of the cross prior to standardization, and B_{std} is the adjust recombination frequency.

TABLE 4

GENETIC RECOMBINATION FREQUENCIES BETWEEN DIFFERENT MHV COMPLEMENTATION GROUPS[a]

Complementation groups	LA3	LA6	LA16	NC2	LA9	LA10	LA18	LA7
A								
LA3	—	0.2 ± .02	0.7 ± 0.1	1.3 ± 0.3	1.6 ± 0.4	5.5 ± 1.5	5.6 ± 0.4	8.5 ± 1.4
LA6	—	—	1.1 ± 0.2	ND	1.9 ± 0.4	5.8 ± 1.5	4.2 ± 0.8	8.6 ± 1.3
LA16	—	—	—	ND	1.3 ± 0.6	2.7 ± 0.3	5.1 ± 1.5	6.2 ± 1.7
B								
NC2	—	—	—	—	1.5 ± 0.5	3.8 ± 1.2	4.3 ± 1.0	6.4 ± 1.8
LA16	—	—	—	ND	1.3 ± 0.6	2.7 ± 0.3	5.1 ± 1.5	6.2 ± 1.7
C								
LA9	—	—	—	—	—	1.4 ± 0.6	3.0 ± 1.8	4.5 ± 0.8
D								
LA10	—	—	—	—	—	—	0.9 ± 0.4	2.6 ± 0.9
E								
LA18	—	—	—	—	—	—	—	1.21 ± 0.3
F								
LA7	—	—	—	—	—	—	—	—

[a] Recombination frequencies were calculated as described in the text.

complementation group were found to map in similar regions of the genetic map. These data suggest that distinct cistrons were encoded in unique regions of the MHV genome. From the 5′ end of the genome, the order of the MHV complementation groups was A, B, C, D, E, and F. Two small regions of overlap were detected between the group A/B and D/E mutants. Mutants within complementation group A mapped over a large domain suggesting that this gene product is very large.

Crosses between ts mutants in the same complementation group had characteristically low recombination frequencies. Not surprisingly, higher recombination frequencies were observed between mutants from different complementation groups and were as high as 8.6%, or 17.2% assuming that crossover events occur in both directions. Since LA7 maps approximately 23–24 kb from the 5′ end of the genome, a 1% recombination frequency occurs over 1300–1400 nucleotides of RNA. Assuming a constant recombination rate through the polymerase region, and that LA6 maps near the 5′ end of the genome, we can utilize the boundaries shown in the recombination map (Fig. 3) to predict the tentative nucleotide domains for each MHV complementation group (Fig. 4). These data predict that the group A mutants map over a 4- to 6-kb stretch of RNA while groups B through E map over smaller domains. While the exact nucleotide domains cannot be predicted from these data, it clearly demonstrates that ts mutants from the same complementation group map in similar nucleotide domains and indicates that all of the RNA$^-$ groups used in this study map in the polymerase gene at the 5′ end of the genome.

DISCUSSION

Homologous recombination has been reported during poliovirus, apthoviruses, and coronavirus infection (Cooper *et al.*, 1975; Cooper, 1977; King *et al.*, 1982, 1985; Lai *et al.*, 1985). For the former viruses, temperature-sensitive mutations in the viral genome have been arranged into a genetic map by recombination analysis (Cooper, 1968; Cooper *et al.*, 1975; Lake *et al.*, 1975). In this report, we demonstrate that complementation groups of MHV-A59 can also be arranged into an additive, linear, genetic map on the basis of their recombination frequencies. This study represents the first report establishing a genetic recombination map for coronaviruses, and provides insight into the approximate number, size, and location of the virus genes which function in RNA synthesis. Moreover, utilizing well-characterized ts mutants, the total recombination frequency for the MHV genome can be predicted.

The MHV genome is divided into seven or eight coding regions (Fig. 4). Expression of each coding region is mediated through the transcription of genome-length or subgenomic mRNA which encode one or more proteins (Siddell, 1983; Spaan *et al.*, 1988). For MHV, eight proteins have been identified which are encoded in subgenomic mRNAs 2 through 7 (Armstrong

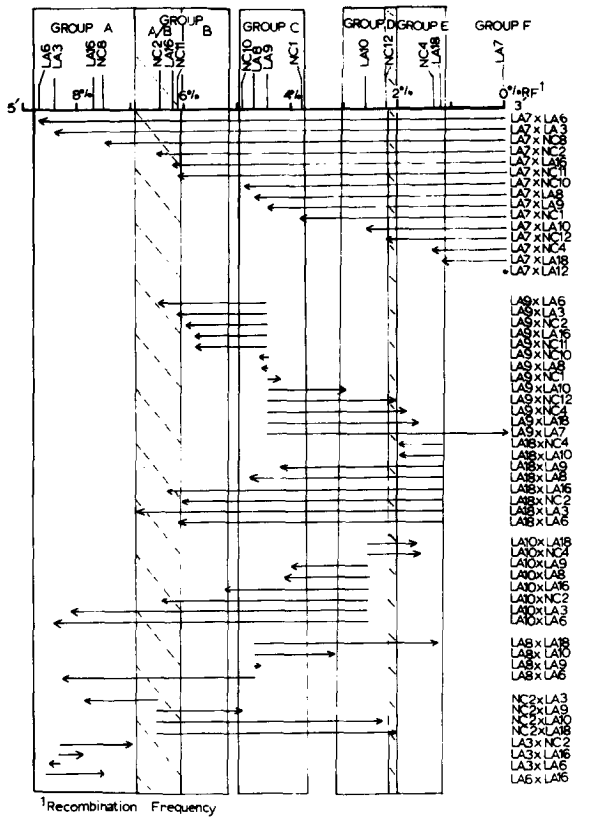

FIG. 3. Genetic recombination map for MHV-A59 complementation groups A through E. Cultures of DBT cells were infected with different combinations of MHV-A59 ts mutants at a m.o.i. of 10 each, and recombination frequencies determined as described under Methods. Percentage recombination frequency is shown across the top of the figure. All mutants were initially positioned with respect to LA7 in the map and the recombination frequencies are shown by the solid arrows. Mutants were then crossed with LA9 and representative mutants from each MHV-A59 complementation group and the boxed areas represent the predicted domains of each complementation group. Hatched domains represent regions of overlap between the group A/B and D/E mutants.

et al., 1984; Schmidt *et al.*, 1987; Shieh *et al.*, 1989; Skinner *et al.*, 1985; Skinner and Siddell, 1983, 1985; Spaan *et al.*, 1988). These include the three structural proteins N, M, and S which are encoded on mRNAs 7, 6, and 3, respectively, and a 43-kDa glycoprotein (HE) encoded in the mRNA 2-1 of some strains of MHV. Four nonstructural proteins are encoded in the subgenomic mRNAs. Viral mRNA2 encodes a 30-kDa nonstructural protein while mRNA 4 is translated into a protein of 15,000 Da molecular weight (p15). Two nonstructural proteins designated p13 and p10 are encoded in two open reading frames on mRNA 5. The function of these nonstructural genes is unknown.

The gene(s) encoded at the 5′ end of the genome is thought to function in regulating RNA synthesis (Spaan *et al.*, 1988). The number of genetic functions encoded in the 23-kb polymerase region is unclear, but this region contains the capacity to encode 700–800 kDa of protein (Pachuk *et al.*, 1989). *In vitro,* the MHV genomic RNA is translated into a 250-kDa precursor polyprotein which is subsequently cleaved into p28 and p220 proteins (Denison and Perlman, 1986, 1987). The p28 protein is encoded within the first 1.1 kb from the 5′ end of the genome (Soe *et al.*, 1987). An autoproteolytic activity, which cleaves the p28 protein from the p250 kilodalton precursor, is encoded 3.9–5.3 kb from the 5′ end of the genome (Baker *et al.*, 1989). Size analysis predicts that the group A mutants map in a cistron which is much larger (4–6 kb) than the domain encoding the p28 protein (1.1 kb).

Several lines of evidence indicate that the increase in ts^+ recombinant progeny that were scored in assays at the nonpermissive temperature represent true recombinants and not aggregates or polyploid particles containing genomes with complementing mutants. First, recombination frequencies are additive and biochemical mapping of several mutants support the location of these cistrons (Keck *et al.*, 1987, 1988c; Lai *et al.*, 1985; Makino *et al.*, 1986b, 1987). Second, the enhancement in the ts^+ recombinant virus yields occur when the parental viruses have defects in the same cistron and are not capable of complementation (Schaad *et al.*, 1990). Third, plaque-purified ts^+ progeny replicate efficiently at permissive and restrictive temperature.

The existence of a genetic map implies that crossovers can occur throughout the MHV genome. Crossover sites in recombinant virus have been demonstrated throughout the MHV genome (Keck *et al.*, 1987, 1988b,c; Lai *et al.*, 1985; Makino *et al.*, 1986b, 1987). Intratypic recombination frequencies between group A and F mutants approach 8.6 or 17.2% assuming that a similar recombination frequency occurs in the opposite direction and results in the double ts phenotype (Table 4). While the double ts mutant recombinant phenotype has not been identified, it seems likely that such recombinants exist. Temperature sensitive mutants mapping internally in the genetic map have additive recombination frequencies with ts mutants mapping in either the 5′ or 3′ direction (Fig. 3). Thus, such mutants probably participate either as an acceptor or donor in template switching to produce recombinant virus. Similar arguments have also been used to predict the total recombination frequencies for the poliovirus and apthovirus genomes (Cooper *et al.*, 1975; King *et al.*, 1987). Since LA7 maps approximately 24 kb from the 5′ end of the 32-kb MHV genome and recombination mapping data predict that complementation group A is too large to map in the p28 protein encoded within the first 1.1 kb from the 5′ end of the genome (Figs. 3 and 4), a 17.2% recombination frequency occurs over

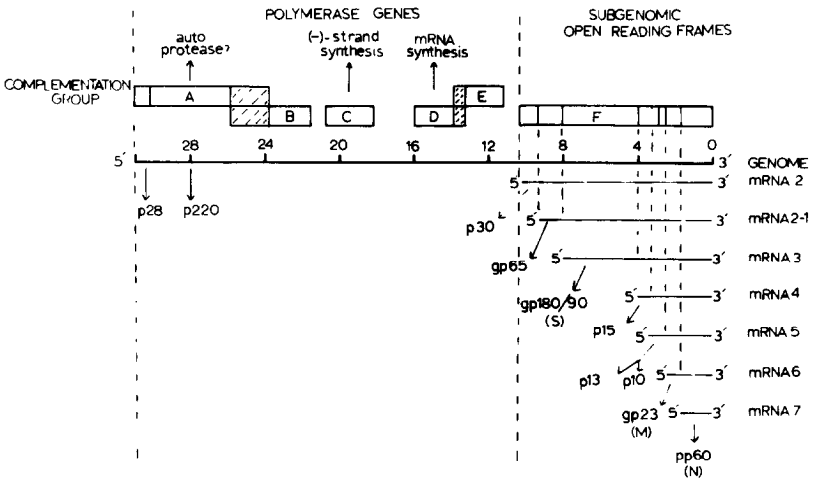

FIG. 4. Tentative map domains for the MHV-A59 complementation groups. The tentative map domains for the MHV-A59 complementation groups were calculated assuming a 1% recombination frequency per 1300 nucleotides of RNA and that LA7 maps 7-8KB from the 3′ end of the genome. The boxed regions represent the approximate size and nucleotide domains of each MHV-A59 complementation group and the probable functions of several groups are predicted. The nucleotide domains and protein products of the subgenomic mRNAs are also shown as well as the putative polymerase products encoded in the genomic RNA. Hatched regions represent areas of overlap between the various complementation groups.

an ~23 kb nucleotide domain or 1%/1300 nucleotides of RNA. If we assume that the recombination frequency over the 5′-most 23 kb is equivalent to the recombination frequency for the 3′-most 8 kb, these data predict that the recombination frequency for the entire ~32-kb MHV genome probably approaches 25% or more, and therefore would be the highest RNA recombination frequency described for a linear plus polarity RNA virus. It seems likely that the predicted recombination frequency probably represents an underestimate since it does not include the frequency of double crossover events (Keck *et al.*, 1988c), the heterogeneity and deletion in the S glycoprotein gene (Parker *et al.*, 1989), the possibility of hot spots of recombination, or crossover events resulting in noninfectious genomes.

Genetic recombination maps between poliovirus ts mutants predict a total recombination frequency of 2.2% over the 7433 nucleotide genome (Cooper *et al.*, 1975; Cooper, 1977; Lake *et al.*, 1975). Assuming that recombination events occur in both directions, these data predict that a 1% recombination frequency occurs per 1700 nucleotide pairs of the poliovirus double-stranded RNA form (Cooper, 1977) and 1%/1300 base pairs for MHV. Recombination frequencies for bacteriophage T4 and *Escherichia coli* are 1%/200 and 1%/1750 base pairs, respectively (Hayes, 1968). Thus, MHV high frequency RNA recombination is probably mediated by the large size of the genomic RNA and a difference in the RNA polymerase molecules of picornaviruses and coronaviruses. This assumption is not surprising since the MHV polymerase probably transcribes leader RNA, dislodges from the template RNA, and reinitiates leader-primed transcription of subgenomic mRNAs from full-length or subgenomic minus strands (Baric *et al.*, 1983, 1985; Makino *et al.*, 1986a; Sawicki and Sawicki, 1990; Sethna *et al.*, 1989). It is unclear why high frequency RNA recombination occurs during mixed MHV infection, but it may provide a mechanism to circumvent potentially high RNA polymerase error rates associated with RNA virus replication (Holland *et al.*, 1982) and a natural source of genetic diversity among coronaviruses (Parker *et al.*, 1989).

Reassortment frequencies for reovirus and influenza virus vary depending on the virus strain and genome segment, and approaches 2–33% and 42%, respectively (Fields, 1981; Scholtissek *et al.*, 1978). Thus, MHV high frequency RNA recombination approaches the reassortment frequency of segmented RNA viruses. The mechanism for MHV high frequency recombination is unclear but may occur as a consequence of discontinuous, nonprocessive transcription during viral replication. If copy choice is the mechanism for MHV recombination, these data suggest that template switching occurs at high frequency. We have previously demonstrated the presence of small RNA intermediates bound to or dissociated from the MHV replicative intermediate RNA (Baric *et al.*, 1983, 1985, 1987). High frequency RNA recombination provides additional evidence that these small RNAs may represent the functional intermediates of RNA transcription and recombination.

Utilizing genetic recombination mapping techniques, we have formulated the first additive, linear, ge-

netic map of the MHV-A59 ts mutants. The orientation of these complementation groups from the 5′ end of the genome was A, B, C, D, E, and F (Figs. 3 and 4). These data are based on two assumptions: (1) that the group A mutant LA6 maps near the 5′ end of the genome and (2) that the recombination frequency is relatively constant over the polymerase region. At this time, it is unclear whether the MHV recombination rate is linear over the length of the genome and this will affect the accuracy of the tentative map domains of the MHV complementation groups. However, the poliovirus and apthovirus recombination maps are linear and appear to represent the physical map locations of ts mutations (King *et al.,* 1987). Complementation groups A, B, C, and D map in the 23-kb polymerase region at the 5′ end of the genome. It also seems likely that the group E mutants map in the polymerase region since these mutants are incapable of transcribing detectable levels of either positive- or negative-stranded RNA at the restrictive temperature (Schaad *et al.,* 1990) and map 5′ to the mRNA 2 coding sequence (Luytjes *et al.,* 1988; Shieh *et al.,* 1989). These data suggest that at least 13 genetic functions are encoded in the MHV genome including five in the polymerase region, two each in mRNAs 2 and 5, and a single genetic function encoded in mRNAs 3, 4, 6, and 7 (Fig. 4). Previous studies with sindbis virus ts mutants indicate that a single complementation group may encode a large multifunctional protein containing two or more functions (Hahn *et al.,* 1989; Mi *et al.,* 1989; Sawicki *et al.,* 1981; Sawicki and Sawicki, 1985). In fact, the nsP2 protein of sindbis is probably involved in the initiation of 26 S RNA synthesis, acting as a protease that cleaves the nonstructural polyprotein precursors, and may be involved in the shutoff of minus-strand RNA synthesis (Sawicki and Sawicki, 1985; Hahn *et al.,* 1989). Since the nucleotide domains of several MHV cistrons appear quite large (3–6 kb), and some mutations within a complementation group map 1300–2600 base pairs apart (group A—LA3/LA6 and NC8/LA16), the MHV complementation groups may also encode multiple functions. This possibility is currently under study.

Previously we have shown that mutants in the group C cistron are probably blocked in the ability to transcribe negative strand RNA while the group D mutants are blocked in the ability to transcribe mRNA, but not leader RNA at restrictive temperature (Baric *et al.,* 1985; Schaad *et al.,* 1990). Mutants from these complementation groups map over internal domains in the polymerase region. The recombination map also predicts that the group A mutants map in the region of the autoproteolytic activity which is encoded ~3.9–5.3 kb from the 5′ end of the genome (Baker *et al.,* 1989). The function of the remaining complementation groups is presently under study. The location of a sixth RNA$^-$ complementation group identified by other investigators is unclear, but could reside in the polymerase region or internally in the viral genome (Koolen *et al.,* 1983; Leibowitz *et al.,* 1982). By size analysis, the group A mutants map over a 4–6 kb nucleotide domain that could encode a protein of approximately 200 kDa molecular weight (Fig. 4). These data suggest that the group A mutants do not map within the p28 protein encoded at the 5′ end of the genome and predict that a sixth genetic function is encoded in this region. Alternatively, an additional genetic function may map internally in the polymerase gene since several large gaps of RNA are present within the genetic map (Fig. 4). Compton *et al.* (1987) have also demonstrated that anti-N monoclonal antibodies block *in vitro* transcription, and we have shown that N is tightly associated with the leader RNA and transcriptional complex (Baric *et al.,* 1988; Stohlman *et al.,* 1988). These data suggest that the N gene functions in RNA transcription and may represent the putative sixth RNA$^-$ complementation group not represented in our panel of ts mutants.

The data presented in this report suggest that the 5′ ~23kb polymerase region of the coronavirus genome contains at least five separate polymerase gene functions that can be ablated by mutagenesis. Although the exact localization of these genetic functions may not be precise, the tentative map domains provide a minimal framework within which to begin characterization of the size, location, and function of the polymerase genes of MHV.

ACKNOWLEDGMENTS

We thank Phyllis Driscoll for excellent technical assistance and Jim Keck and Bob Johnston for helpful comments and criticisms. This investigation was supported by Public Health Service Grants AI 23946 and NS 18146, National Science Foundation Grant DMB-89-17148, and a grant from the American Heart Association (AHA 87-1135). This work was done during the tenure of an Established Investigator of the American Heart Association (AHA 89-0193) (R.S.B.).

REFERENCES

ARMSTRONG, J., NIEMANN, H., SMEEKENS, S., ROTTIER, P., and WARREN, G. (1984). Sequence and topology of a model intracellular membrane protein, E1 glycoprotein, from a coronavirus. *Nature (London)* **308,** 751–752.

BAKER, S. C., SHIEH, C.-K., SOE, L. H., CHANG, M. F., VANNIER, D. M., and LAI, M. M. C. (1989). Identification of a domain required for autoproteolytic cleavage of murine coronavirus gene A polyprotein. *J. Virol.* **63,** 3693–3699.

BARIC, R. S., STOHLMAN, S. A., and LAI, M. M. C. (1983). Characterization of replicative intermediate RNA of mouse hepatitis virus: Presence of leader RNA sequences on nascent chains. *J. Virol.* **48,** 633–640.

BARIC, R. S., STOHLMAN, S. A., RAZAVI, M. K., and LAI, M. M. C. (1985). Characterization of leader-related small RNAs in coronavirus-in-

fected cells: Further evidence for leader-primed mechanism of transcription. *Virus Res.* **3,** 19–33.

BARIC, R. S., SHIEH, C.-K., STOHLMAN, S. A., and LAI, M. M. C. (1987). Analysis of intracellular small RNAs of mouse hepatitis virus: Evidence for discontinuous transcription. *Virology* **156,** 342–354.

BARIC, R. S., NELSON, G. W., FLEMING, J. O., DEANS, R. J., KECK, J. G., CASTEEL, N., and STOHLMAN, S. A. (1988). Interactions between coronavirus nucleocapsid protein and viral RNAs: Implications for viral transcription. *J. Virol.* **62,** 4280–4287.

COMPTON, S. R., ROGERS, D. B., HOLMES, K. V., FERTSCH, D., REMENICK, J., and MCGOWAN, J. J. (1987). In vitro replication of mouse hepatitis virus strain A59. *J. Virol.* **61,** 1814–1820.

COOPER, P. D. (1968). A genetic map of poliovirus temperature-sensitive mutants. *Virology* **35,** 584–596.

COOPER, P. D., STEINER-PRYOR, A., SCOTTI, P. D., and DELONG, D. (1974). On the nature of poliovirus genetic recombinants. *J. Gen. Virol.* **23,** 41–49.

COOPER, P. D., GLEISSLER, E., and TANNOCK, G. A. (1975). Attempts to extend the genetic map of poliovirus temperature-sensitive mutants. *J. Gen. Virol.* **29,** 109–120.

COOPER, P. D. (1977). Genetics of picornaviruses. *In* "Comprehensive Virology," Vol. 9, pp. 133–208. Plenum, New York.

DENISON, M. R., and PERLMAN, S. (1986). Translation and processing of mouse hepatitis virus virion RNA in a cell-free system. *J. Virol.* **60,** 12–18.

DENISON, M., and PERLMAN, S. (1987). Identification of putative polymerase gene product in cells infected with murine coronavirus A59. *Virology* **157,** 565–568.

EPSTEIN, R. H., BOLLE, A., STEINBERG, C. M., KELLENBERGER, C., BOYDE LA TOUR, E., CHEVALLEY, R., EDGAR, R. S., MUSMAN, M., DENHARDT, G. H., and LEILAUSIS, A. (1963). Physiological studies of conditional lethal mutations of bacteriophage T4D. *Cold Spring Harbor Symp. Quant. Biol.* **28,** 374–394.

FENNER, R. (1970). The genetics of animal viruses. *Annu. Rev. Microbiol.* **24,** 297–334.

FIELDS, B. N., and JOKLIK, W. K. (1969). Isolation and preliminary genetic and biochemical characterization of temperature sensitive mutants of reovirus. *Virology* **37,** 335–342.

FIELDS, B. N. (1981). Genetics of Reoviruses. *Curr. Top. Microbiol. Immunol.* **91,** 1–24.

GHENDON, Y. Z. (1972). Conditional-lethal mutants of animal viruses. *Prog. Med. Virol.* **14,** 68–122.

HAHN, Y. S., STRAUSS, E. G., and STRAUSS, J. H. (1989). Mapping of RNA$^-$ temperature sensitive mutants of sindbis virus: Assignment of complementation groups A, B, and G to nonstructural proteins. *J. Virol.* **63,** 3142–3150.

HAYES, W. (1968). *In* "The Genetics of Bacteria and Their Viruses," 2nd ed. Blackwell, Oxford.

HOLLAND, J., SPINDLER, K., HORODYSKI, F., GRABAU, E., NICHOL, S., and VANDEPOL, S. (1982). Rapid evolution of RNA genomes. *Science* **215,** 1577–1585.

KECK, J. G., STOHLMAN, S. A., SOE, L. H., MAKINO, S., and LAI, M. M. C. (1987). Multiple recombination sites at the 5′ end of the murine coronavirus RNA. *Virology* **156,** 331–341.

KECK, J. G., HOGUE, B. G., BRIAN, D. A., and LAI, M. M. C. (1988a). Temporal regulation of bovine coronavirus RNA synthesis. *Virus. Res.* **9,** 343–356.

KECK, J. G., MATSUSHIMA, G. K., MAKINO, S., FLEMING, J. O., VANNIER, D. M., STOHLMAN, S. A., and LAI, M. M. C. (1988b). In vivo RNA–RNA recombination of coronavirus in mouse brain. *J. Virol.* **62,** 1810–1813.

KECK, J. G., SOE, L. H., MAKINO, S., STOHLMAN, S. A., and LAI, M. M. C. (1988c). RNA recombination of murine coronaviruses: Recombination between fusion-positive mouse hepatitis virus A59 and fusion-negative mouse hepatitis virus 2. *J. Virol.* **62,** 1989–1998.

KING, A. M., MCCAHON, D., SLADE, W. R., and NEWMAN, J. W. I. (1982). Recombination in RNA. *Cell* **29,** 921–928.

KING, A. M. Q., MCCAHON, D., SAUNDERS, K., NEWMAN, J. W. I., and SLADE, W. R. (1985). Multiple sites of recombination within the RNA genome of foot-and-mouth disease virus. *Virus Res.* **3,** 373–384.

KING, A. M. Q., ORTLEPP, S. A., NEWMAN, J. W., and MCCAHON, D. (1987). Genetic recombination in RNA viruses. *In* "The Molecular Biology of the Positive Strand RNA Viruses" (R. J. Rowlands, M. A. Mayo, and B. N. Mahy, Eds.), pp. 129–152. Academic Press, London.

KIRKEGAARD, K., and BALTIMORE, D. (1986). The mechanism of RNA recombination in poliovirus. *Cell* **47,** 433–443.

KOOLEN, M. J. M., OSTERHAUS, A. D. M. E., VAN STEENIS, G., HORZINEK, M. C., and VAN DER ZEIJST, B. A. M. (1983). Temperature-sensitive mutants of mouse hepatitis virus strain A59: Isolation, characterization and neuropathogenic properties. *Virology* **125,** 393–402.

LAI, M. M. C., BARIC, R. S., MAKINO, S., KECK, J. G., EGBERT, J., LEIBOWITZ, J. L., and STOHLMAN, S. A. (1985). Recombination between nonsegmented RNA genomes of murine coronavirus. *J. Virol.* **56,** 449–456.

LAKE, J. R., PRISTON, R. A. J., and SLADE, W. R. (1975). A genetic recombination map of foot-and-mouth disease virus. *J. Gen. Virol.* **27,** 355–367.

LEIBOWITZ, J. L., DE VRIES, J. R., and HASPEL, M. V. (1982). Genetic analysis of murine hepatitis virus strain JHM. *J. Virol.* **42,** 1080–1087.

LUYTJES, W., BREDENBEEK, P. J., NOTEN, A. F., HORZINEK, M. C., and SPAAN, W. J. (1988). Sequence of mouse hepatitis virus A59 mRNA2: Indications for RNA-recombination between coronaviruses and influenza C virus. *Virology* **166,** 415–422.

MACKENZIE, J. S., SLADE, W. R., LAKE, J., PRISTON, R. A., BISBY, J., LAING, S., and NEWMAN, J. (1975). Temperature-sensitive mutants of foot and mouth disease virus: The isolation of mutants and observations on their properties and genetic recombination. *J. Gen. Virol.* **27,** 61–70.

MAKINO, S., STOHLMAN, S. A., and LAI, M. M. C. (1986a). Leader sequences of murine coronavirus mRNAs can be freely reassorted: Evidence for the role of free leader RNA in transcription. *Proc. Natl. Acad. Sci. USA* **83,** 4204–4208.

MAKINO, S., STOHLMAN, S. A., and LAI, M. M. C. (1986b). High frequency RNA recombination of murine coronaviruses. *J. Virol.* **57,** 328–334.

MAKINO, S., FLEMING, J. O., KECK, J. G., STOHLMAN, S. A., and LAI, M. M. C. (1987). RNA recombination of coronaviruses; localization of neutralizing epitopes and neuropathogenic determinants on the carboxy terminus of peplomers. *Proc. Natl. Acad. Sci. USA* **84,** 6567–6571.

MARTIN, J. P., KOEHREN, F., RANNOU, J.-J., and KIRN, A. (1988). Temperature sensitive mutants of mouse hepatitis virus type 3(MHV-3): Isolation, biochemical and genetic characterization. *Arch. Virol.* **100,** 147–160.

MI, S., DURBIN, R., HUANG, H. V., RICE, C. M., and STOLLAR, V. (1989). Association of the sindbis virus RNA methyltransferase activity with the nonstructural protein nsP1. *Virology* **170,** 385–391.

PACHUK, C. J., BREDENBECK, P. J., ZOLTICK, P. W., SPAAN, W. J. M., and WEISS, S. R. (1989). Molecular cloning of the gene encoding the putative polymerase of mouse hepatitis coronavirus, strain A59. *Virology* **171,** 141–148.

PARKER, S. E., GALLAGHER, T. M., and BUCHMEIER, M. J. (1989). Sequence analysis reveals extensive polymorphism and evidence of

deletions within the E2 glycoprotein gene of several strains of murine hepatitis virus. *Virology* **173,** 664–673.

RITCHIE, D. A. (1973). Genetic analysis of animal viruses. *Brit. Med. J.* **29,** 947–952.

SAWICKI, D. L., SAWICKI, S. G., KERANEN, S., and KAARIAINEN, L. (1981). Specific sindbis virus coded function for minus strand RNA synthesis. *J. Virol.* **39,** 348–358.

SAWICKI, D. L., and SAWICKI, S. G. (1985). Functional analysis of the A complementation group mutants of Sindbis HR virus. *Virology* **144,** 20–34.

SAWICKI, S. G., and SAWICKI, D. L. (1990). Coronavirus transcription: Subgenomic mouse hepatitis virus replicative intermediates function in RNA synthesis. *J. Virol.* **64,** 1050–1056.

SCHAAD, M. C., STOHLMAN, S. A., EGBERT, J., LUM, K., FU, K., WEI, T., and BARIC, R. S. (1990). Genetics of mouse hepatitis virus transcription: Identification of cistrons which may function in positive and negative strand RNA synthesis. *Virology* **177,** 634–645.

SCHMIDT, I., SKINNER, M. A., and SIDDELL, S. G. (1987). Nucleotide sequence of the gene encoding the surface projection glycoprotein of coronavirus MHV-JHM. *J. Gen. Virol.* **68,** 47–56.

SCHOLTISSEK, C., RHODE, W., VON HOYNINGEN, V. V., and ROTT, R. (1978). On the origin of the human influenza virus subtypes H2N2 and H3N2. *Virology* **87,** 13–20.

SETHNA, P. B., HUNG, S. L., and BRIAN, D. A. (1989). Coronavirus subgenomic minus-strand RNAs and the potential for mRNA replicons. *Proc. Natl. Acad. Sci. USA* **86,** 5626–5630.

SHIEH, C.-K., LEE, H.-J., YOKOMORI, K., LA MONICA, N., MAKINO, S., and LAI, M. M. C. (1989). Identification of a new transcriptional initiation site and the corresponding functional gene 2b in the murine coronavirus RNA genome. *J. Virol.* **63,** 3729–3736.

SIDDELL, S. (1983). Coronavirus JHM: Coding assignments of subgenomic mRNAs. *J. Gen. Virol.* **64,** 113–125.

SKINNER, M. A., and SIDDELL, S. G. (1983). Coronavirus JHM nucleotide sequence of the mRNA that encodes the nucleocapsid protein. *Nucleic Acid Res.* **11,** 5045–5054.

SKINNER, M. A., EBNER, D., and SIDDELL, S. G. (1985). Coronavirus MHV-JHM mRNA 5 has a sequence arrangement which potentially allows translation of a second, downstream open reading frame. *J. Gen. Virol.* **66,** 581–592.

SKINNER, M. A., and SIDDELL, S. G. (1985). Coding sequence of coronavirus MHV-JHM mRNA 4. *J. Gen. Virol.* **66,** 581–592.

SOE, L. H., SHIEH, C. K., BAKER, S. C., CHANG, M. F., and LAI, M. M. C. (1987). Sequence and translation of the murine coronavirus 5′-end genomic RNA reveals the N-terminal structure of the putative RNA polymerase. *J. Virol.* **61,** 3968–3976.

SPAAN, W. J. M., CAVANAGH, D., and HORZINEK, M. C. (1988). Coronaviruses: Structure and genome expression. *J. Gen. Virol.* **69,** 2939–2952.

STOHLMAN, S. A., BARIC, R. S., NELSON, G. N., SOE, L. H., WELTER, L. M., and DEANS, R. J. (1988). Specific interaction between the coronavirus leader RNA and nucleocapsid protein. *J. Virol.* **62,** 4288–4295.